

REMARKS ON DISCRETIZATIONS OF CONVECTION TERMS IN HYBRID MIMETIC MIXED METHODS

JÉRÔME DRONIOU

Université Montpellier 2
Institut de Mathématiques et de Modélisation de Montpellier, CC 051
Place Eugène Bataillon
34095 Montpellier cedex 5, France

ABSTRACT. We present different ways, coming from Finite Volume or Mixed Finite Element frameworks, to discretize convection terms in Hybrid Finite Volume, Mimetic Finite Difference and Mixed Finite Volume methods for elliptic equations. We compare them through several numerical tests, deducing some generic principles, depending on the situation, on the choice of an appropriate method and its parameters. We also present an adaptation to the Navier-Stokes equations, with a numerical tests in the case of the lid-driven cavity.

1. Introduction. The Hybrid Finite Volume (HFV), Mimetic Finite Difference (MFD) and Mixed Finite Volume (MFV) methods, developed in the last few years, aim at providing numerical schemes on very generic grids for diffusion equations of the kind

$$\begin{cases} -\operatorname{div}(\Lambda \nabla p) = f & \text{in } \Omega, \\ p = 0 & \text{on } \partial\Omega, \end{cases} \quad (1)$$

where Ω is a polygonal open bounded subset of \mathbf{R}^d ($d \geq 2$) and $\Lambda : \Omega \rightarrow \mathbf{R}^{d \times d}$ is a bounded uniformly coercive (and usually symmetric) tensor.

These three methods basically come from two different communities: the Mixed Finite Element community (MFD) and the Finite Volume community (HFV, MFV). It has recently been understood [9] that they are in fact only different presentations, based on the different takes and habits of each community, of a single discretization technique, which can be named the “Hybrid Mimetic Mixed” (HMM) method.

Diffusion terms of the kind $\operatorname{div}(\Lambda \nabla p)$ appear in numerous models of physical problems, and their discretization on general grids is a complex problem which alone justifies a large literature on development of methods for the plain diffusion equation (1). But many such models (the Navier-Stokes equations, miscible or immiscible flows in porous media, etc.) also involve convection terms, and it is therefore important not only to study discretizations of pure diffusion equations, but also to gather some understanding on how to handle convection-diffusion equations,

2000 *Mathematics Subject Classification.* Primary: 65N12, 65N30, 65M12, 65M60.

Key words and phrases. Mixed finite volume, Hybrid finite volume, Mimetic finite difference, Hybrid Mixed Mimetic method, convection-diffusion equation, convection-dominated problems, elliptic-parabolic coupled problems, flow in porous media.

This work was supported by GnR MoMaS CNRS/PACEN and Project VFSitCom (ANR-08-BLAN-0275-01).

the model of those being

$$\begin{cases} -\operatorname{div}(\Lambda \nabla p) + \operatorname{div}(Vp) = f & \text{in } \Omega, \\ p = 0 & \text{on } \partial\Omega \end{cases} \quad (2)$$

with $V \in C^1(\overline{\Omega})^d$ (since this equation is stationary, as usual we assume that $\operatorname{div}(V) \geq 0$). Of course, the discretization of $\operatorname{div}(Vp)$ is not expected to be something as complex as the discretization of $\operatorname{div}(\Lambda \nabla p)$, but it is well known that convection-diffusion equations can be quite tricky to properly approximate: different treatments of the convective term can be required depending on which process (the convection or the diffusion) dominates.

Mixed Finite Element and Finite Volume literatures both have developed techniques to handle convective terms; the HMM method being at the juncture of these two literatures, it can be written in either one format and this mutability thus allows to try and incorporate into HMM schemes all those different handling of convection terms. The aim of this paper is precisely to present couplings of the HMM technique for pure diffusion equations with several FE or FV discretizations of convection terms.

The plan is as follows: in the next section, we recall the HMM discretization of pure diffusion equations (1), using two of its possible presentations (MFD and MFV) associated with the FE and FV views of the method. In Section 3, we use these two presentations to couple the HMM method with FE- or FV-based discretizations of the convective term, thus obtaining several schemes for the convection-diffusion equation (2); we very briefly state the theoretical results which can be proved on these schemes, the details being provided in [2]. In Section 4 we present some numerical comparisons between these methods. The results are on the overall what is expected, but some interesting insights can nevertheless be gained (for example, on the scaling of the Scharfetter-Gummel method, or on the choice of cell or edge unknowns in the upwindings). The model equation (2), although sometimes difficult to properly approximate, is a very simple convection-diffusion problem, which can however give pretty good ideas on how to discretize, using HMM methods, more complex convection-diffusion problems also involving heterogeneous and anisotropic data (see e.g. [7], in which a slight variant of the HMM method has been applied to a model of miscible flows in porous media). In Section 5, we present HMM discretizations of the Navier-Stokes equation, which also involves diffusion and convection terms; the classical situations of study of the Navier-Stokes equations only involve a homogeneous and isotropic diffusion term, but the model is a system of equation in which convective term is quite different from the one in (2) (being strongly non-linear), and some behaviors displayed by the solutions are quite different from the ones which can be seen on the solutions to (2); a quick study of a classical test case (the lid driven cavity) therefore appears interesting to have a better grasp of the strengths and weaknesses of the various HMM discretizations we consider in this work. Some concluding remarks are gathered in the last section of the paper.

2. The HMM discretization of pure diffusion equations.

2.1. Notations. The following definition gives the basic notations for the grids we consider on Ω .

Definition 2.1. An admissible discretization of Ω is given by the triplet $\mathcal{D} = (\mathcal{M}, \mathcal{E}, \mathcal{P})$, where :

- \mathcal{M} , the cells (or control volumes) of the mesh, is a finite family of non-empty open polygonal disjoint subsets of Ω such that $\overline{\Omega} = \cup_{K \in \mathcal{M}} \overline{K}$;
- \mathcal{E} , the edges (faces in 3D) of the mesh, is a finite family of non-empty open disjoint subsets σ of $\overline{\Omega}$ such that for all $\sigma \in \mathcal{E}$ there exists an affine hyperplane \mathcal{A} of \mathbf{R}^d and a cell $K \in \mathcal{M}$ such that $\sigma \subset \partial K \cap \mathcal{A}$. We also assume that for all $K \in \mathcal{M}$ there exists $\mathcal{E}_K \subset \mathcal{E}$ such that $\partial K = \cup_{\sigma \in \mathcal{E}_K} \sigma$ and, for all $\sigma \in \mathcal{E}$, either $\sigma \subset \partial\Omega$ or $\sigma \in \mathcal{E}_K \cap \mathcal{E}_L$ for some pair of elements $K, L \in \mathcal{M}$;
- $\mathcal{P} = (x_K)_{K \in \mathcal{M}}$ is a family of points of Ω indexed by \mathcal{M} , such that each mesh cell K is star-shaped with respect to x_K .

The set of edges σ contained in $\partial\Omega$ is denoted by \mathcal{E}_{ext} , and we let $\mathcal{E}_{\text{int}} = \mathcal{E} \setminus \mathcal{E}_{\text{ext}}$ denote the interior edges. Two control volumes K and L which share an edge are called neighbors; $|K|$ and $|\sigma|$ respectively denote the d -dimensional and the $(d-1)$ -dimensional measures of the cell K and the edge σ . If $\sigma \in \mathcal{E}_K$, $\mathbf{n}_{K,\sigma}$ is the unit normal to σ outward K .

We define $H_{\mathcal{M}}$ as the set of functions $\Omega \rightarrow \mathbf{R}$ which are piecewise constant on \mathcal{M} (the value of $q \in H_{\mathcal{M}}$ on K is denoted by q_K), and $\mathcal{F}_{\mathcal{D}}$ is the set of families of real numbers $(F_{K,\sigma})_{K \in \mathcal{M}, \sigma \in \mathcal{E}_K}$ which satisfy the following conservativity property:

$$\text{for all } K \text{ and } L \text{ neighbors, for all } \sigma \in \mathcal{E}_K \cap \mathcal{E}_L : F_{K,\sigma} + F_{L,\sigma} = 0. \quad (3)$$

2.2. Scheme. The HMM method for the diffusion equation (1) can be introduced in three different but equivalent ways [9], coming from three different points of view: in a manner similar to the Mixed Finite Element method (MFD), using a variational formulation of the problem based on discrete gradients (HFV) or writing a flux-based finite volume formulation (MFV). We briefly describe here the first and third presentations, which will be useful to introduce the various discretizations of the convection term in the next section, and we refer the reader to [4, 9, 10, 13] for more detailed constructions of the method.

In the MFD view of the HMM method, a discrete divergence operator is first defined: for all $G \in \mathcal{F}_{\mathcal{D}}$, $\mathcal{DIV}(G) \in H_{\mathcal{M}}$ is given by

$$(\mathcal{DIV}(G))_K = \frac{1}{|K|} \sum_{\sigma \in \mathcal{E}_K} |\sigma| G_{K,\sigma}$$

and, for each control volume K , a local scalar product $[\cdot, \cdot]_K$, acting on the restrictions to \mathcal{E}_K of elements in $\mathcal{F}_{\mathcal{D}}$, is chosen such that the following consistency property holds (this is the discrete counterpart of the usual Stokes formula):

$$\forall G \in \mathcal{F}_{\mathcal{D}}, \forall q \text{ affine function} :$$

$$[(\Lambda_K \nabla q)^I, G]_K + \int_K q (\mathcal{DIV}(G))_K = \sum_{\sigma \in \mathcal{E}_K} G_{K,\sigma} \int_{\sigma} q, \quad (4)$$

where $\Lambda_K = \frac{1}{|K|} \int_K \Lambda$ and the interpolation \mathbf{w}^I of a sufficiently regular vector field \mathbf{w} is defined by $(\mathbf{w})^I_{K,\sigma} = \frac{1}{|\sigma|} \int_{\sigma} \mathbf{w} \cdot \mathbf{n}_{K,\sigma}$.

Remark 2.2. To prove the convergence of the method, the local scalar products $[\cdot, \cdot]_K$ are also assumed to satisfy the following estimates:

$$\forall G \in \mathcal{F}_{\mathcal{D}}, \forall K \in \mathcal{M} : C_* \sum_{\sigma \in \mathcal{E}_K} |K| (G_{K,\sigma})^2 \leq [G, G]_K \leq C^* \sum_{\sigma \in \mathcal{E}_K} |K| (G_{K,\sigma})^2 \quad (5)$$

with $C^*, C_* > 0$ not depending on the mesh in the family along which the convergence is studied.

Defining the scalar product $[\cdot, \cdot]_{\mathcal{F}_D}$ on \mathcal{F}_D as the sum of all the local scalar products, i.e. $[F, G]_{\mathcal{F}_D} = \sum_{K \in \mathcal{M}} [F, G]_K$, and $[\cdot, \cdot]_{H_{\mathcal{M}}}$ as the usual $L^2(\Omega)$ scalar product, the HMM scheme for (1) consists in writing a Mixed Finite Element-like formulation using these scalar products: find $(p, F) \in H_{\mathcal{M}} \times \mathcal{F}_D$ such that

$$\forall G \in \mathcal{F}_D : [F, G]_{\mathcal{F}_D} - [p, \mathcal{DIV}(G)]_{H_{\mathcal{M}}} = 0, \quad (6)$$

$$\forall q \in H_{\mathcal{M}} : [\mathcal{DIV}(F), q]_{H_{\mathcal{M}}} = (f, q)_{L^2(\Omega)}. \quad (7)$$

As with the classical Mixed Finite Element method, it is possible to hybridize this scheme by introducing edge unknowns $p_{\mathcal{E}} = (p_{\sigma})_{\sigma \in \mathcal{E}}$ (local eliminations then allow to write the entire system using only $p_{\mathcal{E}}$). These edge unknowns are useful to present the MFV approach of the HMM method; we first define a discrete cell gradient from the fluxes:

$$\mathbf{v}_K(F) = -\frac{1}{|K|} \Lambda_K^{-1} \sum_{\sigma \in \mathcal{E}_K} |\sigma| F_{K,\sigma} (\bar{x}_{\sigma} - x_K), \quad (8)$$

where \bar{x}_{σ} is the center of gravity of σ (and x_K is the point corresponding to the chosen discretization \mathcal{D} of Ω); if $F_{K,\sigma}$ is an approximation of $\frac{1}{|\sigma|} \int_{\sigma} -\Lambda \nabla p \cdot \mathbf{n}_{K,\sigma}$, then $\mathbf{v}_K(F)$ is indeed an approximation of ∇p on K . Letting $H_{\mathcal{E},0}$ be the space of edge values $q_{\mathcal{E}} = (q_{\sigma})_{\sigma \in \mathcal{E}}$ such that $q_{\sigma} = 0$ whenever $\sigma \in \mathcal{E}_{\text{ext}}$, the HMM scheme consists in imposing a relation inside each cell between the flux, cell and edge unknowns, and in writing the physical flux balance: find $(p, p_{\mathcal{E}}, F) \in H_{\mathcal{M}} \times H_{\mathcal{E},0} \times \mathcal{F}_D$ such that

$$\begin{aligned} \forall K \in \mathcal{M}, \forall G \in \mathcal{F}_D : & \sum_{\sigma \in \mathcal{E}_K} |\sigma| G_{K,\sigma} (p_K - p_{\sigma}) \\ & = |K| \mathbf{v}_K(F) \cdot \Lambda_K \mathbf{v}_K(G) + T_K(G)^T \mathbb{B}_K T_K(F), \end{aligned} \quad (9)$$

$$\forall K \in \mathcal{M} : \sum_{\sigma \in \mathcal{E}_K} |\sigma| F_{K,\sigma} = \int_K f, \quad (10)$$

where $T_K(F) = (T_{K,\sigma}(F))_{\sigma \in \mathcal{E}_K}$ with $T_{K,\sigma}(F) = F_{K,\sigma} + \Lambda_K \mathbf{v}_K(F) \cdot \mathbf{n}_{K,\sigma}$ and \mathbb{B}_K is a symmetric positive definite matrix of size $\text{Card}(\mathcal{E}_K)$ (we see that $T_K(F) = 0$ whenever $(F_{K,\sigma})_{\sigma \in \mathcal{E}_K}$ are the genuine fluxes of a given vector ξ , i.e. $F_{K,\sigma} = \Lambda_K \xi \cdot \mathbf{n}_{K,\sigma}$, and the term $T_K(G)^T \mathbb{B}_K T_K(F)$ is thus a stabilization term which vanishes as F approximates the genuine fluxes of the exact solution).

Remark 2.3. Rigorously speaking, (6)–(7) and (9)–(10) are equivalent only if the points $(x_K)_{K \in \mathcal{M}}$ are chosen as the centers of gravity of the cells. In general, (4) has to be generalized a little bit in order to preserve the equivalence; this generalization is at the core of the unified HMM view of the method, see [9].

3. Various discretizations of the convection term.

3.1. Using mixed finite element techniques. A first idea to discretize the convective term in (1) is to put this equation into a mixed weak formulation; $H(\text{div}, \Omega)$ being the classical space of square-integrable vector fields with square-integrable divergence, a weak formulation for (2) is: find $(p, F) \in L^2(\Omega) \times H(\text{div}, \Omega)$ such that

$$\begin{aligned} \forall \mathbf{w} \in H(\text{div}, \Omega) : & (\Lambda^{-1} F, \mathbf{w})_{L^2(\Omega)} - (p, \text{div}(\mathbf{w}))_{L^2(\Omega)} \\ & - (\Lambda^{-1} V p, \mathbf{w})_{L^2(\Omega)} = 0, \end{aligned} \quad (11)$$

$$\forall q \in L^2(\Omega) : (\text{div}(F), q)_{L^2(\Omega)} = (f, q)_{L^2(\Omega)} \quad (12)$$

(the first equation states that $F = -\Lambda \nabla p + Vp$, and the second equation that $\operatorname{div}(F) = f$).

If \mathbf{w} and \mathbf{z} are regular vector fields then, taking $G = \mathbf{w}^I$ and q an affine function such that $\nabla q = \Lambda_K^{-1} \frac{1}{|K|} \int_K \mathbf{z}$ in (4), since $(\mathcal{DIV}(G))_K = \frac{1}{|K|} \int_K \operatorname{div}(\mathbf{w}) = \operatorname{div}(\mathbf{w}) + \mathcal{O}(\operatorname{diam}(K))$ on K , we obtain, thanks to (5),

$$[\mathbf{z}^I, \mathbf{w}^I]_K + \int_K q \operatorname{div}(\mathbf{w}) + \mathcal{O}(|K| \operatorname{diam}(K)) = \sum_{\sigma \in \mathcal{E}_K} G_{K,\sigma} \int_{\sigma} q = \sum_{\sigma \in \mathcal{E}_K} \int_{\sigma} \mathbf{w} \cdot \mathbf{n}_{K,\sigma} q(\bar{x}_{\sigma})$$

(we use the fact that q is affine, so that $\int_{\sigma} q = |\sigma| q(\bar{x}_{\sigma})$). Integrating by part the second term, we find

$$[\mathbf{z}^I, \mathbf{w}^I]_K = \int_K \nabla q \cdot \mathbf{w} + \sum_{\sigma \in \mathcal{E}_K} \int_{\sigma} \mathbf{w} \cdot \mathbf{n}_{K,\sigma} (q(\bar{x}_{\sigma}) - q) + \mathcal{O}(|K| \operatorname{diam}(K)).$$

We then notice that $\nabla q = \Lambda_K^{-1} \mathbf{z} + \mathcal{O}(\operatorname{diam}(K))$ on K , that $\mathbf{w} = \mathbf{w}(\bar{x}_{\sigma}) + \mathcal{O}(\operatorname{diam}(K))$ and $q(\bar{x}_{\sigma}) - q = \mathcal{O}(\operatorname{diam}(K))$ on σ , that $|\sigma| \operatorname{diam}(K) = \mathcal{O}(|K|)$ and that $\int_{\sigma} (q(\bar{x}_{\sigma}) - q) = 0$ to obtain

$$[\mathbf{z}^I, \mathbf{w}^I]_K = \int_K \Lambda_K^{-1} \mathbf{z} \cdot \mathbf{w} + \mathcal{O}(|K| \operatorname{diam}(K)).$$

Assuming that Λ is constant inside each control volume K , this justifies the following approximation of the convective term in (11):

$$(\Lambda^{-1} Vp, \mathbf{w})_{L^2(\Omega)} = \sum_{K \in \mathcal{M}} \int_K \Lambda_K^{-1} Vp \cdot \mathbf{w} \approx \sum_{K \in \mathcal{M}} p_K \int_K \Lambda_K^{-1} V \cdot \mathbf{w} \approx \sum_{K \in \mathcal{M}} p_K [V^I, G]_K$$

where we have taken $G = \mathbf{w}^I$.

The resulting HMM scheme for the full equation (2), proposed and studied in [5], is then: find $(p, F) \in H_{\mathcal{M}} \times \mathcal{F}_{\mathcal{D}}$ such that

$$\forall G \in \mathcal{F}_{\mathcal{D}} : [F, G]_{\mathcal{F}_{\mathcal{D}}} - [p, \mathcal{DIV}(G)]_{H_{\mathcal{M}}} - \sum_{K \in \mathcal{M}} p_K [V^I, G]_K = 0, \tag{13}$$

$$\forall q \in H_{\mathcal{M}} : [\mathcal{DIV}(F), q]_{H_{\mathcal{M}}} = (f, q)_{L^2(\Omega)}. \tag{14}$$

It has been proved in [5] that, under usual assumptions on the grid regularity and if the solution to (2) belongs to $H^2(\Omega)$, an order 1 error estimate for p and the fluxes holds in natural norms (the L^2 norm for the p , the norm on $\mathcal{F}_{\mathcal{D}}$ induced by $[\cdot, \cdot]_{\mathcal{F}_{\mathcal{D}}}$ for the fluxes). Moreover, under stronger regularity assumptions on the grid, domain, source and velocity terms, a superconvergence of p can also be theoretically proved.

In case of strong convection, it turns out that (13)–(14), though still theoretically convergent, can provide very oscillating solutions on coarse meshes. It is then possible to improve its behaviour by adding a stabilization term which consists in penalizing the jumps of the solution: we define $J_{\mathcal{D}}(p) \in H_{\mathcal{M}}$ by

$$J_{\mathcal{D}}(p)_K = \frac{\zeta}{2|K|} \sum_{\sigma \in \mathcal{E}_K} |\sigma| |(V^I)_{K,\sigma}| (p_K - p_L)$$

(where L is the cell on the other side of σ , and $p_L = 0$ if $\sigma \in \mathcal{E}_{\text{ext}}$), with $\zeta > 0$ which can be chosen in order to control the strength of the penalization, and we replace (14) with

$$\forall q \in H_{\mathcal{M}} : [\mathcal{DIV}(F) + J_{\mathcal{D}}(p), q]_{H_{\mathcal{M}}} = (f, q)_{L^2(\Omega)}. \tag{15}$$

Obviously, the choice $\zeta = 0$ gives back the original method (13)–(14).

3.2. Using finite volume techniques. The principle of Finite Volume discretizations of the term $\operatorname{div}(Vp)$ in (2) is to integrate it on a cell and use Stokes' formula:

$$\int_K \operatorname{div}(Vp) = \sum_{\sigma \in \mathcal{E}_K} \int_{\sigma} pV \cdot \mathbf{n}_{K,\sigma} =: \sum_{\sigma \in \mathcal{E}_K} |\sigma| F_c(p)_{K,\sigma}.$$

The next step is to approximate $F_c(p)_{K,\sigma} = \frac{1}{|\sigma|} \int_{\sigma} pV \cdot \mathbf{n}_{K,\sigma}$ using the available unknowns, i.e. the cell unknowns $(p_K)_{K \in \mathcal{M}}$ in general; there are several possible classical choices. In the following, we let $V_{K,\sigma} = \frac{1}{|\sigma|} \int_{\sigma} V \cdot \mathbf{n}_{K,\sigma}$ and denote by L the control volume on the other side of $\sigma \in \mathcal{E}_K$ (or $p_L = 0$ if $\sigma \in \mathcal{E}_K \cap \mathcal{E}_{\text{ext}}$).

- Centered flux:

$$F_c(p)_{K,\sigma} = V_{K,\sigma} \frac{p_K + p_L}{2}. \quad (16)$$

- Upwind flux:

$$F_c(p)_{K,\sigma} = \begin{cases} V_{K,\sigma} p_K & \text{if } V_{K,\sigma} \geq 0, \\ V_{K,\sigma} p_L & \text{if } V_{K,\sigma} < 0. \end{cases} \quad (17)$$

- Scharfetter-Gummel flux, scaled with the local diffusion:

$$F_c(p)_{K,\sigma} = \frac{\mu_{\sigma}}{d_{\sigma}} \left[A \left(\frac{d_{\sigma}}{\mu_{\sigma}} V_{K,\sigma} \right) p_K - A \left(-\frac{d_{\sigma}}{\mu_{\sigma}} V_{K,\sigma} \right) p_L \right] \quad (18)$$

where d_{σ} is the sum of the orthogonal distances between σ and x_K and between σ and x_L , $A(s) = \frac{e^{-s}}{e^{-s}-1} - 1$ and $\mu_{\sigma} = \min(1, \min\{\operatorname{Sp}(\Lambda_K) \cup \operatorname{Sp}(\Lambda_L)\})$ (see Sections 4.1 and 4.2.2 for some comments on the use of μ_{σ} as a scaling parameter).

A HMM scheme for (2) can then be obtained from (9)–(10) by adding the convective fluxes to the flux balance equation: find $(p, p_{\mathcal{E}}, F) \in H_{\mathcal{M}} \times H_{\mathcal{E},0} \times \mathcal{F}_{\mathcal{D}}$ such that

$$\begin{aligned} \forall K \in \mathcal{M}, \forall G \in \mathcal{F}_{\mathcal{D}}: \quad & \sum_{\sigma \in \mathcal{E}_K} |\sigma| G_{K,\sigma} (p_K - p_{\sigma}) \\ & = |K| \mathbf{v}_K(F) \cdot \Lambda_K \mathbf{v}_K(G) + T_K(G)^T \mathbb{B}_K T_K(F), \end{aligned} \quad (19)$$

$$\forall K \in \mathcal{M}: \quad \sum_{\sigma \in \mathcal{E}_K} |\sigma| (F_{K,\sigma} + F_c(p)_{K,\sigma}) = \int_K f, \quad (20)$$

with F_c defined by one of the preceding choices (16), (17) or (18).

All these expressions of the convective fluxes use the two values on either side of σ as in the classical 2-point Finite Volume method (in which the primary unknowns are the cell unknowns, see [12]). However, as noticed above, HMM methods naturally provide an unknown for p on each edge, which could be used instead of the cell unknown on the other side; for example, in the case of an upwind discretization, the discrete convective flux (17) can be replaced with

$$F_c(p, p_{\mathcal{E}})_{K,\sigma} = \begin{cases} V_{K,\sigma} p_K & \text{if } V_{K,\sigma} \geq 0, \\ V_{K,\sigma} p_{\sigma} & \text{if } V_{K,\sigma} < 0 \end{cases} \quad (21)$$

(edge-based variants of the centered and Scharfetter-Gummel discretizations (16) and (18) can also be devised). Whereas the fluxes (17) are conservative, this is not the case for the fluxes $F_c(p, p_{\mathcal{E}})$ defined by (21); since the conservativity of the global (diffusive+convective) fluxes is still expected to hold, (3) has to be relaxed

and, with the choice (21), the HMM scheme is thus: find $(p, p_{\mathcal{E}}) \in H_{\mathcal{M}} \times H_{\mathcal{E},0}$ and a set of real numbers $F = (F_{K,\sigma})_{K \in \mathcal{M}, \sigma \in \mathcal{E}_K}$ such that

$$\begin{aligned} &\forall K, L \text{ neighboring cells, } \forall \sigma \in \mathcal{E}_K \cap \mathcal{E}_L : \\ &F_{K,\sigma} + F_c(p, p_{\mathcal{E}})_{K,\sigma} + F_{L,\sigma} + F_c(p, p_{\mathcal{E}})_{L,\sigma} = 0, \end{aligned} \tag{22}$$

$$\begin{aligned} &\forall K \in \mathcal{M}, \forall (G_{K,\sigma})_{\sigma \in \mathcal{E}_K} \in \mathbf{R}^{\text{Card}(\mathcal{E}_K)} : \\ &\sum_{\sigma \in \mathcal{E}_K} |\sigma| G_{K,\sigma} (p_K - p_{\sigma}) = |K| \mathbf{v}_K(F) \cdot \Lambda_K \mathbf{v}_K(G) + T_K(G)^T \mathbb{B}_K T_K(F), \end{aligned} \tag{23}$$

$$\forall K \in \mathcal{M} : \sum_{\sigma \in \mathcal{E}_K} |\sigma| (F_{K,\sigma} + F_c(p, p_{\mathcal{E}})_{K,\sigma}) = \int_K f. \tag{24}$$

3.3. A word on the theoretical study. As shown in [2], all these HMM schemes for convection-diffusion equations (i.e. the stabilized MFE-based scheme [(13),(15)], the FV-based methods with cell unknowns (19)–(20) and the FV-based methods with cell and edge unknowns (22)–(24)) can be written in a unified presentation which allows to make a single theoretical study encompassing them all, and other possible methods.

In particular, theoretical proofs of convergence (without regularity assumption on the solution to the PDE) and first order error estimates (when the solution to the PDE belongs to H^2) are established in [2], under usual assumptions on the grids.

4. Numerical results. We provide here some numerical results on the schemes, some of them leading to what we believe to be interesting and new comments on some choices of the discretization of the convection term.

4.1. Orders of convergence. Some rates of convergence for the preceding methods are provided in [2], but only in the case of isotropic and homogeneous cases ($\Lambda = \nu \text{Id}$ and V constant). We complete here those results by looking at the rates of convergence in the following anisotropic heterogeneous case: we consider (2) with

- $\Omega = (0, 1)^2$,
- $\Lambda(x, y)$ the diffusion tensor given by a $2\pi x$ rotation of the diagonal matrix $\nu \text{diag}(2, 1)$ for some $\nu > 0$, i.e.

$$\begin{aligned} \Lambda(x, y) = & \\ & \nu \begin{pmatrix} \cos(2\pi x) & -\sin(2\pi x) \\ \sin(2\pi x) & \cos(2\pi x) \end{pmatrix} \begin{pmatrix} 2 & 0 \\ 0 & 1 \end{pmatrix} \begin{pmatrix} \cos(2\pi x) & -\sin(2\pi x) \\ \sin(2\pi x) & \cos(2\pi x) \end{pmatrix}^{-1}, \end{aligned} \tag{25}$$

- V the divergence-free vector field $V(x, y) = 10(-y, x)$,
- f the source term corresponding to the exact solution $p(x, y) = x(1-x)e^y$.

If ν is not small (say $\nu = 1$), this problem is mostly in diffusive regime; for small ν , the convection dominates. We implement the schemes using refinements of the grid presented in Figure 1-(a): each primordial, triangular or quadrangular, cell is divided into a certain number of cells of the same nature, obtained by cutting each edge into n segments; Figure 1-(b) shows the refinement corresponding to $n = 10$ (the grids used in the tests correspond to $n = 25, n = 50, n = 100, n = 150$ and $n = 200$ and are respectively made of 5625, 22500, 90000, 202500 and 360000 cells).

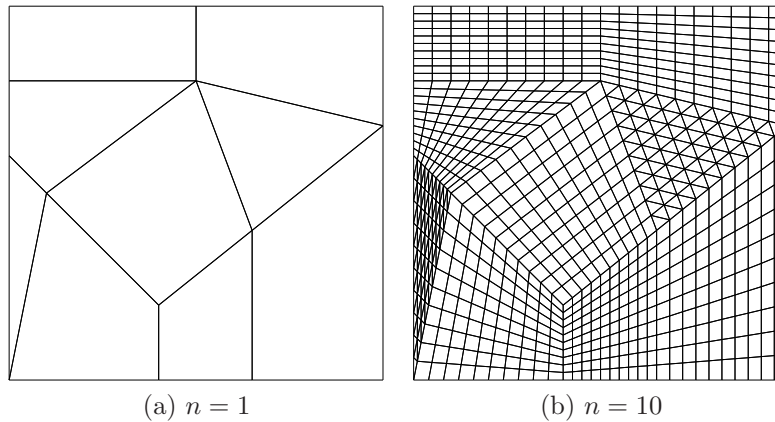


FIGURE 1. Two elements of the family of grids used to compute the rates of convergence.

The quantities of interest are the relative errors e_p and $e_{\nabla p}$, in L^2 norms, of p and ∇p , i.e.

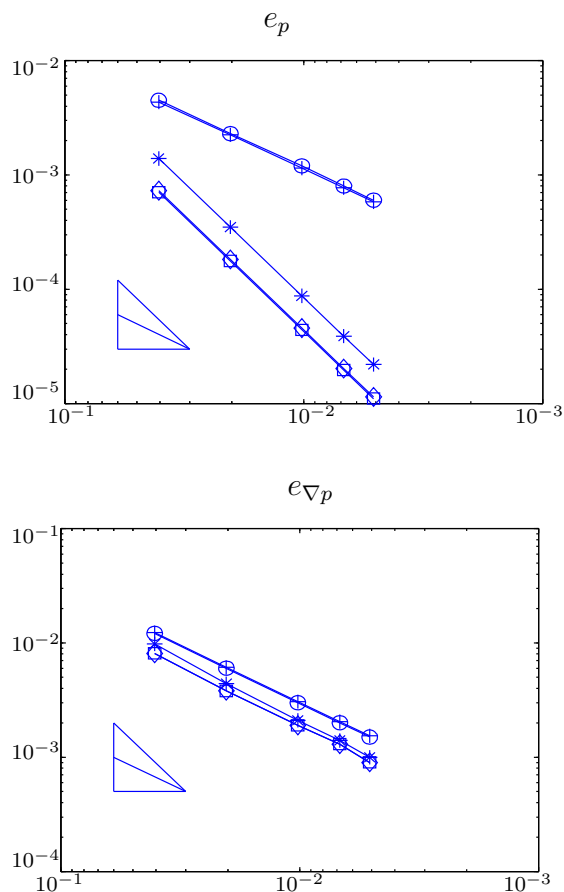
$$e_p = \frac{\|p - \bar{p}_{\mathcal{M}}\|_{L^2(\Omega)}}{\|\bar{p}_{\mathcal{M}}\|_{L^2(\Omega)}} \quad \text{and} \quad e_{\nabla p} = \frac{\|\mathbf{v}(F) - (\nabla \bar{p})_{\mathcal{M}}\|_{L^2(\Omega)}}{\|(\nabla \bar{p})_{\mathcal{M}}\|_{L^2(\Omega)}}$$

where p is the approximate piecewise constant solution given by the considered scheme, $\bar{p}_{\mathcal{M}} = (\bar{p}(x_K))_{K \in \mathcal{M}}$ and $(\nabla \bar{p})_{\mathcal{M}} = (\nabla \bar{p}(x_K))_{K \in \mathcal{M}}$ are piecewise constant projections of the exact solution to (2) and its gradient, and $\mathbf{v}(F)$ is the approximate gradient defined by (8).

In Figure 2 we present the convergence graphs obtained in the diffusive regime $\nu = 1$, with various discretizations of the convection: the FV-upwind method based on (21), the FV-Scharfetter-Gummel method based on the edge-version of (18) (i.e. with p_L replaced by p_σ), the FV-centered method based on (16) but also replacing p_L with p_σ , the FE-like method (13)–(14) and the stabilized FE-like method [(13), (15)] with $\zeta = 1$.

These results show a super-convergence (order 2) of p for all the schemes except the FV-upwind scheme and the stabilized FE-like scheme (which only exhibits an order 1 convergence), and an order 1 convergence of the discrete gradient for all the schemes. Other test cases in diffusive regime give similar outputs, but the relative positions of the three schemes showing a superconvergence for p may change (in a numerical test of [2], the FE-like discretization gives slightly better results than the two others). These behaviors are somewhat expected, and correspond to what is observed when these techniques of discretization of the convective term are used alongside other kinds of schemes for diffusion operators.

In Figure 3, we present the results in the convection-dominated case: we take $\nu = 10^{-4}$ in (25). Here again, the results correspond to the expectations: the FV-centered discretization nearly provides, as the mesh size goes to 0, a second order of convergence for p , but with very large errors, whereas the FV-upwind and stabilized FE-like schemes still have a convergence rate of order 1, but gives an acceptable numerical solution. Also as expected, the convergence of the approximate gradient is very slow at the available mesh sizes.



Legend: \circ FV-upwind, \square FV-Scharfetter-Gummel, \diamond FV-centered, \star FE-like, $+$ stabilized FE-like.

FIGURE 2. Rates of convergence in the diffusive regime ($\nu = 1$ in (25)): graph in log-log scale of the errors with respect to the size h of the mesh (reference slopes: h and h^2).

Remark 4.1. We do not include, in the convective regime, the results obtained with the non-stabilized FE-like method since the corresponding scheme gives a very unstable solution (the error is huge on the the grids we consider here)

A more interesting remark can be made on the Scharfetter-Gummel discretization: the corresponding solution is nearly indistinguishable from the solution provided by the upwind scheme; this is in fact completely natural if we remember the definition of the scaling parameter μ_σ in (18): we have

$$\frac{\mu_\sigma}{d_\sigma} A \left(\frac{d_\sigma}{\mu_\sigma} s \right) = \frac{-s}{\exp(-\frac{d_\sigma}{\mu_\sigma} s) - 1} - \frac{\mu_\sigma}{d_\sigma}$$

and hence, if $\mu_\sigma/d_\sigma \ll 1$ ⁽¹⁾,

$$\frac{\mu_\sigma}{d_\sigma} A \left(\frac{d_\sigma}{\mu_\sigma} s \right) \approx \begin{cases} s & \text{if } s > 0, \\ 0 & \text{if } s < 0. \end{cases}$$

This shows that, in this strongly convective regime, the fluxes (18) and (17) are nearly identical.

The scaled Scharfetter-Gummel flux therefore appears as a very good “generic” choice for the discretization of the convective term: when the diffusion dominates, it gives an order 2 scheme similar to the centered methods (Figure 2) and, when the convection takes over, it provides enough numerical diffusion to stabilize the solution, as with the upwind choice (Figure 3).

Additional numerical tests are available in [2]. The results presented in this reference do not show the convergence graphs of the approximate gradient, but rather study the rates of convergence of the flux unknowns (in the \mathcal{F}_D norm) and show, in some cases, a super-convergence phenomenon (order of convergence 3/2 instead of 1) for these unknowns.

Remark 4.2. The approximation of the gradient in the convective regime is quite bad: Figure 3 shows that the best relative errors are around 1, which means that a 100% error is made on the approximation of ∇p . The cause is the following: the approximate gradient $\mathbf{v}(F)$ is constructed using the diffusive fluxes but, in the convective regime, these diffusive fluxes are very small with respect to the convective fluxes, and are therefore badly approximated by the numerical scheme (they nearly only represent “noise” around the large convective fluxes).

However, from the physical point of view, and keeping in mind some possible coupling of equations (as in complex models of flows in porous media for example), the total (diffusive+convective) fluxes seem to be the important quantity to properly approximate, and the results in [2] show that, even in convective regime, these total fluxes are well approximated by the upwind and stabilized HMM methods.

4.2. Qualitative behavior.

4.2.1. *Qualitative test 1.* In this test, we consider the anisotropic heterogeneous discontinuous diffusion tensor

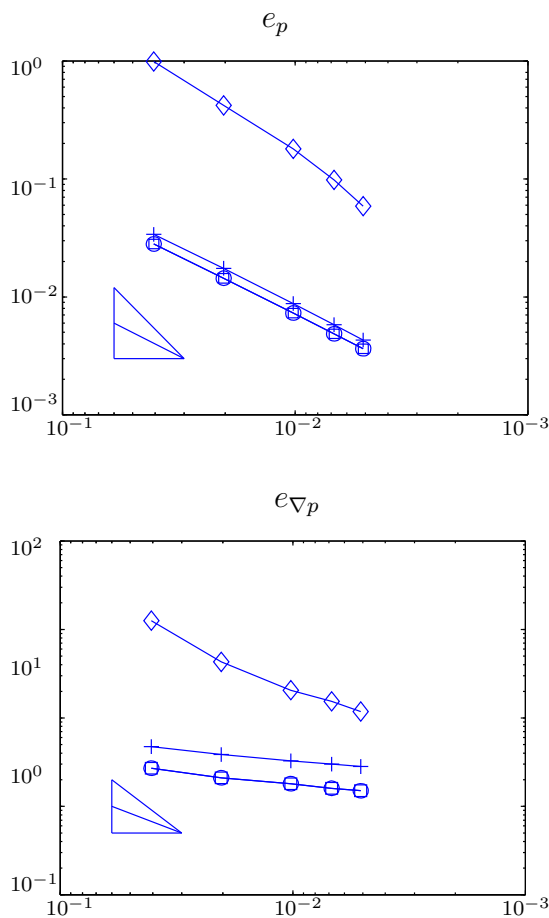
$$\Lambda = \begin{pmatrix} 1 & 0 \\ 0 & 1 \end{pmatrix} \text{ on } (0, 0.5) \times (0, 1), \quad \Lambda = \begin{pmatrix} 1 & 0 \\ 0 & 10^{-6} \end{pmatrix} \text{ on } (0.5, 1) \times (0, 0.5)$$

and $\Lambda = \begin{pmatrix} 10^{-6} & 0 \\ 0 & 1 \end{pmatrix} \text{ on } (0.5, 1) \times (0.5, 1),$

with the constant convection field $V = (5, 0)$; the source f is equal to 1 on $(0.2, 0.4) \times (0.2, 0.8)$ and to 0 elsewhere on the domain $\Omega = (0, 1)^2$. This test case presents a change of regime: if $x \leq 0.5$ or $y \leq 0.5$, the phenomenon is mainly diffusion-dominated (even in the lower right quarter of domain, since both the diffusion tensor and the convection field are large along the x -axis and small along the y -axis), but it shifts to a convective regime on the upper right domain $(0.5, 1) \times (0.5, 1)$ (the convection is strong in the x -axis, along which the diffusion is very small).

The exact solution, or rather its approximation obtained on a very fine cartesian grid, is shown in Figure 4-(a); due to the definition of Λ , this solution is nearly discontinuous on the line $(0.5, 1) \times \{0.5\}$. In the same figure, (c) and (d) show the

¹which is the case here for the considered grids, since $\mu_\sigma = 10^{-4}$ and the smallest grid size is 5×10^{-3} .



Legend: \circ FV-upwind, \square FV-Scharfetter-Gummel, \diamond FV-centered, $+$ stabilized FE-like.

FIGURE 3. Rates of convergence in the convective regime ($\nu = 10^{-4}$ in (25)): graph in log-log scale of the errors with respect to the size h of the mesh (reference slopes: h and h^2).

approximate solution obtained, on the grid made of a 25×25 reproduction of the pattern showed in (b), with the HMM scheme using the FV cell- or edge-upwind discretizations of the convection term (i.e. with the choice (17) or (21)).

The results clearly show that, although based on similar principles, these two kinds of upwind discretizations can have quite different behaviors: the cell-upwind choice appears much less precise than the edge-upwind choice. As a general rule, we noticed on different numerical tests on the HMM discretization of (2) that either these two choices give very similar results, or the edge-upwind discretization is better than the cell-upwind discretization.

Remark 4.3. Another advantage of the edge-upwind choice, with respect to the cell-upwind choice, is the possibility to fully hybridize (22)–(24) (the system can be reduced, via local eliminations, to a system in the edge unknowns only).

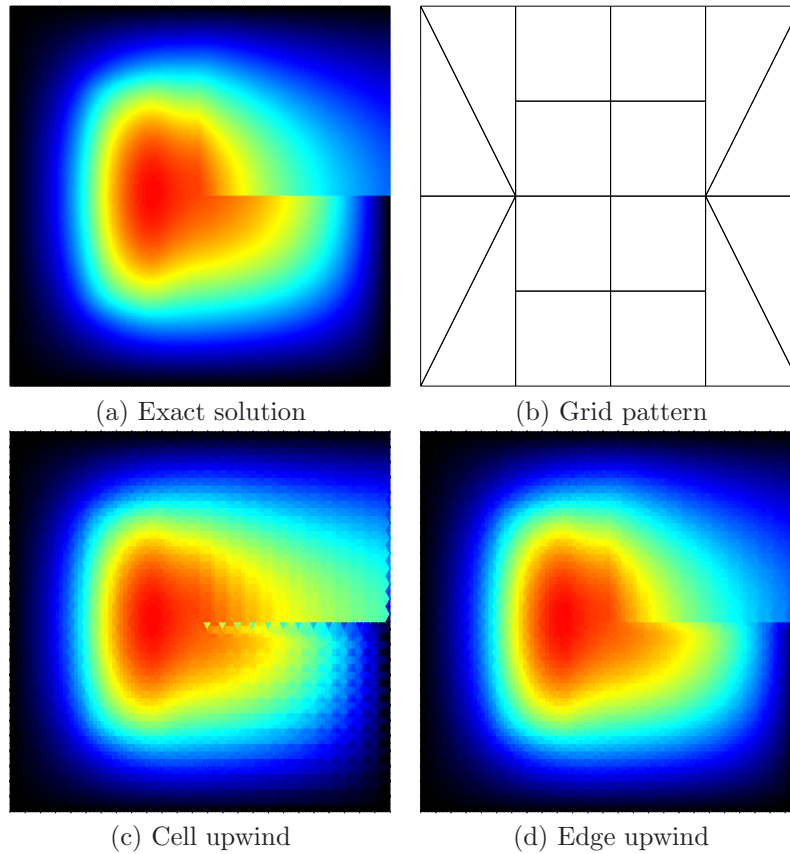


FIGURE 4. Qualitative test 1, with a change of regime: comparison between the cell and edge upwind choices (the approximate solutions (c) and (d) are obtained on the grid made of a 25×25 reproduction of the pattern (b)).

4.2.2. *Qualitative test 2.* In this test, we study in more depth the scaling used in the Scharfetter-Gummel convective flux (18).

The Scharfetter-Gummel scheme has been developed for an homogeneous isotropic material ($\Lambda = \text{Id}$), in dimension 1 or for the standard 2-point Finite Volume scheme, to give a simultaneous approximation of the diffusion and convection fluxes [16, 6]. One can extract a “purely convective” flux from this method by considering the 2-point Finite Volume Scharfetter-Gummel schme for $-\Delta p + \text{div}(Vp) = f$ and crudely removing the 2-point approximation of the diffusive flux: this leads to taking

$$F_c(p)_{K,\sigma} = \frac{1}{d_\sigma} (A(-d_\sigma V_{K,\sigma}) p_K - A(d_\sigma V_{K,\sigma}) p_L). \quad (26)$$

However, this simple construction is completely unstable in convection-dominated cases and it has to be scaled using some coefficient μ_σ , which takes into account the local diffusivity of the PDE, and writing (18) instead of (26). As we saw above, if μ_σ is close to 0, its use ensures that the Scharfetter-Gummel method nearly boils down to an upwind (and thus very stable, although quite diffusive) scheme.

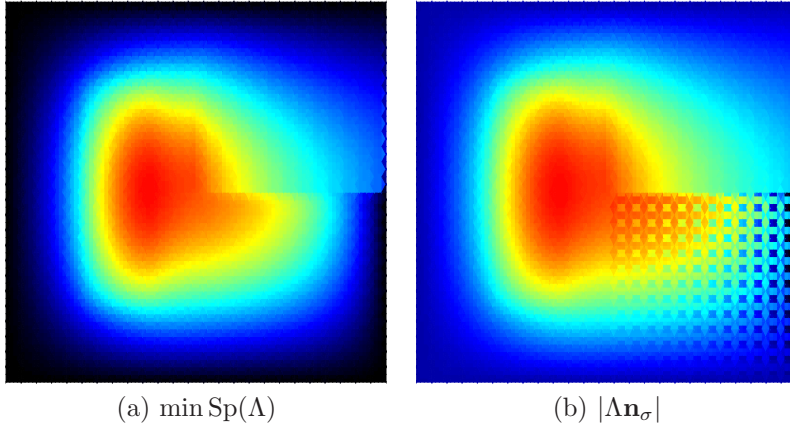


FIGURE 5. Qualitative test 2, with two possible stabilizations of the Scharfetter-Gummel method: using the smallest local eigenvalue of Λ , or $|\Lambda \mathbf{n}_\sigma|$ (same data and grid as in the qualitative test 1).

A simple reasoning shows that μ_σ ought to be of the same magnitude as Λ ⁽²⁾, but even then the precise expression of μ_σ is quite free, and not necessarily obvious to choose in order to obtain enough but not too much numerical diffusion in a HMM method for an anisotropic operator on a generic grid.

The choice $\mu_\sigma = \min(1, \min(\text{Sp}(\Lambda_K) \cup \text{Sp}(\Lambda_L)))$ of the smallest local eigenvalue of Λ is a “safe bet” since it consists in considering that the worst possible situation occurs (Λ brings its smallest possible diffusion in the flux across σ); a finer way to tune μ_σ would be to consider that the strength of the diffusion brought by Λ to the fluxes across σ is of order $|\Lambda \mathbf{n}_\sigma|$, and thus to take $\mu_\sigma = \min(1, |\Lambda_K \mathbf{n}_{K,\sigma}|, |\Lambda_L \mathbf{n}_{L,\sigma}|)$ as a sufficient “upwinding” of the Scharfetter-Gummel initial convective flux. As it turns out, this is not a good choice: Figure 5 shows the results obtained, using the same data as the qualitative test 1, by using either one or the other choice for μ_σ ; these results clearly indicate that a stabilization using only the magnitude of Λ in the orthogonal direction of σ can be insufficient to stabilize the scheme in the convective-dominated region.

This can be explained by the following heuristic: the reasoning “the strength of the diffusion brought by Λ to the fluxes across σ is of order $|\Lambda \mathbf{n}_\sigma|$ ” used above is correct for the 2-point Finite Volume scheme, for which (on an admissible grid as in [12]) the diffusive flux can be written

$$F_{K,\sigma} = |\sigma| \frac{\lambda_K \lambda_L}{d(x_L, \sigma) \lambda_K + d(x_K, \sigma) \lambda_L} (p_K - p_L)$$

with $\lambda_K = |\Lambda_K \mathbf{n}_{K,\sigma}|$ and $\lambda_L = |\Lambda_L \mathbf{n}_{L,\sigma}|$. Hence, for the 2-point scheme, λ_K and λ_L give a good estimate of the magnitude of the natural diffusion in the scheme, and thus probably a good lead to determine “how much” numerical diffusion has to be artificially added (through the use of μ_σ) to the Scharfetter-Gummel discretization

²Consider $-\varepsilon \Delta p + \text{div}(Vp) = f$, divide this equation by ε , write the 2-point Finite Volume Scharfetter-Gummel scheme for $-\Delta p + \text{div}(\frac{V}{\varepsilon} p) = \frac{f}{\varepsilon}$ and multiply the resulting scheme by ε to obtain a scheme for $-\varepsilon \Delta p + \text{div}(Vp) = f$: this leads to choosing (18) with $\mu_\sigma = \varepsilon$.

of the convective term in order to stabilize the global method. But for HMM schemes, the expression of the diffusive flux is less straightforward and involves all the directions, not only the orthogonal direction to the edge: (9) shows that the expression of $F_{K,\sigma}$ involves all the $(p_K - p_{\sigma'})_{\sigma' \in \mathcal{E}_K}$, not only $p_K - p_{\sigma \dots}$.

5. Application to Navier-Stokes equations. It might be interesting to look at the various discretization of convection terms in HMM schemes for more complex problems than the pure convection-diffusion equation. The upwind technique, for example, has been used in conjunction with a variant of the HMM method (replacing $T_K(F)$ by F_K and choosing a diagonal \mathbb{B}_K in (9)) in [7] for a non-linear elliptic-parabolic system of equations modeling miscible flows in porous media; this situation is quite close to the one described by our basic equation (2), and the conclusions of the previous numerical tests can give pretty good insights on how to choose the discretization of the convection term, depending on the expected regime.

We want to study here the previous HMM methods for a different kind of non-linear model, involving diffusion and convection operators but in an isotropic homogeneous situation and leading to quite different behaviors than the behaviors displayed by the solution to (2): the Navier-Stokes equation

$$\begin{cases} -\Delta \mathbf{u} + (\mathbf{u} \cdot \nabla) \mathbf{u} + \nabla p = \mathbf{f} & \text{in } \Omega, \\ \operatorname{div}(\mathbf{u}) = 0 & \text{in } \Omega, \\ \mathbf{u} = 0 & \text{on } \partial\Omega, \\ \int_{\Omega} p = 0, \end{cases} \quad (27)$$

where $\mathbf{u} : \Omega \rightarrow \mathbf{R}^d$ is the velocity field and $p : \Omega \rightarrow \mathbf{R}$ the pressure (we present the equation with an homogeneous boundary condition for simplicity).

The same variant as above of the HMM method has been used in [11] to discretize this equation (and its transient form), using a kind of centered discretization of the non-linear convective term $(\mathbf{u} \cdot \nabla) \mathbf{u}$, but it is quite easy to write the genuine HMM scheme for this equation, using any of the techniques from Section 3 for the discretization of the non-linear term. The presentation of this method for Navier-Stokes equations, and above all the numerical study of various possible choices for the discretization of the convective term, is not made in [2] or [11] and some of the conclusions we draw below are therefore new.

Remark 5.1. Note that it is possible to modify, at some cost (large stencil, some instabilities in case of heterogeneities...), the HMM method in order to obtain a cell-centered scheme; it has been done in [13] for the pure scalar diffusion equation, and in [8] for the Navier-Stokes equation, with two possible choices for the discretization of the convection term (centered or upwind, but all other choices are easily usable).

5.1. The discretization. The unknowns associated with the HMM discretization of (27) are the cell and edge vector velocities $\mathbf{u} = (\mathbf{u}_K)_{K \in \mathcal{M}} \in H_{\mathcal{M}}^d$ and $\mathbf{u}_{\mathcal{E}} = (\mathbf{u}_{\sigma})_{\sigma \in \mathcal{E}} \in H_{\mathcal{E},0}^d$, the vector velocity fluxes $\mathbf{F} = (\mathbf{F}_{K,\sigma})_{K \in \mathcal{M}, \sigma \in \mathcal{E}_K} \in \mathcal{F}_{\mathcal{D},\text{nc}}^d$ and the scalar pressure $p = (p_K)_{K \in \mathcal{M}} \in H_{\mathcal{M}}$ (we denote by $\mathcal{F}_{\mathcal{D},\text{nc}}$ the space of *possibly non-conservative* families of real numbers $(F_{K,\sigma})_{K \in \mathcal{M}, \sigma \in \mathcal{E}_K}$). The link between the discrete velocity and its fluxes is made by using the matrices

$$\mathbf{v}_K(\mathbf{F}_K) = -\frac{1}{|K|} \sum_{\sigma \in \mathcal{E}_K} |\sigma| \mathbf{F}_{K,\sigma} \otimes (\bar{x}_{\sigma} - x_K)$$

and by writing

$$\begin{aligned} \forall K \in \mathcal{M}, \forall \mathbf{G} \in \mathcal{F}_{\mathcal{D},\text{nc}}^d : \sum_{\sigma \in \mathcal{E}_K} |\sigma| \mathbf{G}_{K,\sigma} \cdot (\mathbf{u}_\sigma - \mathbf{u}_K) \\ = \sum_{i=1}^d \left(\mathbf{v}_K(\mathbf{F}_K)_i \cdot \mathbf{v}_K(\mathbf{G}_K)_i + T_K((\mathbf{G}_K)_i)^T \mathbb{B}_{K,i} T_K((\mathbf{F}_K)_i) \right) \end{aligned} \quad (28)$$

where $\mathbf{v}_K(\mathbf{F}_K)_i$ is the i -th line of the matrix $\mathbf{v}_K(\mathbf{F}_K)$, $T_K((\mathbf{F}_K)_i) = ((\mathbf{F}_{K,\sigma})_i + \mathbf{v}_K(\mathbf{F}_K)_i \cdot \mathbf{n}_{K,\sigma})_{\sigma \in \mathcal{E}}$ and $\mathbb{B}_{K,i}$ is a symmetric positive definite $\text{Card}(\mathcal{E}_K) \times \text{Card}(\mathcal{E}_K)$ matrix.

The incompressibility condition $\text{div}(\mathbf{u}) = 0$ is translated in the discrete setting by integrating it on each cell, which leads to impose

$$\forall K \in \mathcal{M} : \sum_{\sigma \in \mathcal{E}_K} |\sigma| \mathbf{u}_\sigma \cdot \mathbf{n}_{K,\sigma} = 0 \quad (29)$$

and the normalization condition $\int_\Omega p = 0$ is simply written

$$\sum_{K \in \mathcal{M}} |K| p_K = 0. \quad (30)$$

The discretization of the momentum equation in (27), which consists in writing the balance of forces on a cell, is

$$\forall K \in \mathcal{M} : \sum_{\sigma \in \mathcal{E}_K} (|\sigma| \mathbf{F}_{K,\sigma} + |\sigma| p_K \mathbf{n}_{K,\sigma}) + \sum_{\sigma \in \mathcal{E}_K} |\sigma| \mathbf{F}_c^{\mathbf{u}_\sigma \cdot \mathbf{n}}(\mathbf{u}, \mathbf{u}_\mathcal{E})_{K,\sigma} = \int_K \mathbf{f}. \quad (31)$$

The first sum in this equation comes from the diffusive term and the pressure $-\Delta \mathbf{u} + \nabla p$, whereas the second is the discretization of the non-linear term $(\mathbf{u} \cdot \nabla) \mathbf{u}$, in which $\mathbf{F}_c^{\mathbf{u}_\sigma \cdot \mathbf{n}}(\mathbf{u}, \mathbf{u}_\mathcal{E})$ is some numerical convective flux function, chosen amongst the possibilities presented in Section 3 (e.g. FE-like – with or without stabilization –, centered, upwind, Scharfetter-Gummel, and in each case using either the cell or edge variant) and constructed using $\mathbf{u}_\sigma \cdot \mathbf{n}_{K,\sigma}$ instead of $V_{K,\sigma}$ (the first \mathbf{u} in “ $(\mathbf{u} \cdot \nabla) \mathbf{u}$ ” plays the role of V in $\text{div}(V\mathbf{u})$). For example, the stabilized FE-like discretization with cell values leads to

$$\mathbf{F}_c^{\mathbf{u}_\sigma \cdot \mathbf{n}}(\mathbf{u}, \mathbf{u}_\mathcal{E})_{K,\sigma} = \left(\mathbf{u}_\sigma \cdot \mathbf{n}_{K,\sigma} + \frac{\zeta}{2} |\mathbf{u}_\sigma \cdot \mathbf{n}_{K,\sigma}| \right) \mathbf{u}_K - \frac{\zeta}{2} |\mathbf{u}_\sigma \cdot \mathbf{n}_{K,\sigma}| \mathbf{u}_L,$$

the centered discretization with cell values is

$$\mathbf{F}_c^{\mathbf{u}_\sigma \cdot \mathbf{n}}(\mathbf{u}, \mathbf{u}_\mathcal{E})_{K,\sigma} = \mathbf{u}_\sigma \cdot \mathbf{n}_{K,\sigma} \frac{\mathbf{u}_K + \mathbf{u}_L}{2} \quad (32)$$

(this is the one used in [11]) and the Scharfetter-Gummel choice with edge upwinding is

$$\mathbf{F}_c^{\mathbf{u}_\sigma \cdot \mathbf{n}}(\mathbf{u}, \mathbf{u}_\mathcal{E})_{K,\sigma} = \frac{1}{d_\sigma} (A(d_\sigma \mathbf{u}_\sigma \cdot \mathbf{n}_{K,\sigma}) \mathbf{u}_K - A(-d_\sigma \mathbf{u}_\sigma \cdot \mathbf{n}_{K,\sigma}) \mathbf{u}_\sigma)$$

with the same function $A(s) = \frac{-s}{e^{-s}-1} - 1$ as above.

We finally impose the continuity (or conservativity) of the global fluxes appearing in (31):

$$\begin{aligned} \forall \sigma \in \mathcal{E}_{\text{int}} : (\mathbf{F}_{K,\sigma} + p_K \mathbf{n}_{K,\sigma} + \mathbf{F}_c^{\mathbf{u}_\sigma \cdot \mathbf{n}}(\mathbf{u}, \mathbf{u}_\mathcal{E})_{K,\sigma}) \\ + (\mathbf{F}_{L,\sigma} + p_L \mathbf{n}_{L,\sigma} + \mathbf{F}_c^{\mathbf{u}_\sigma \cdot \mathbf{n}}(\mathbf{u}, \mathbf{u}_\mathcal{E})_{L,\sigma}) = 0 \end{aligned} \quad (33)$$

where, as usual, K and L are the cells on either side of σ .

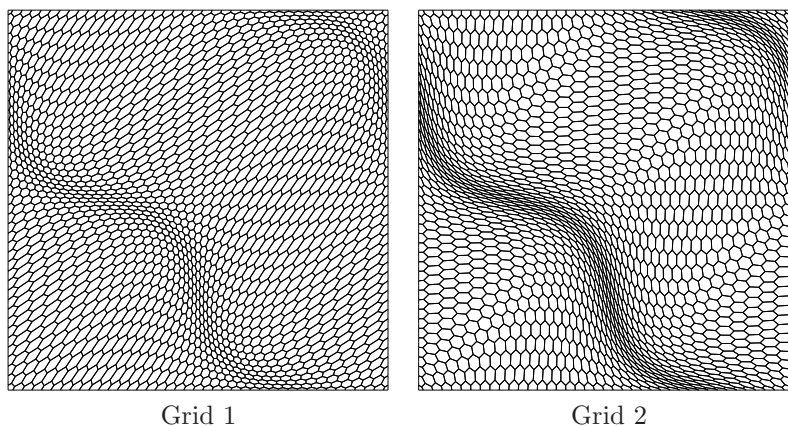


FIGURE 6. Grids used for the tests, on the lid-driven cavity case, of the HMM method for Navier-Stokes equations.

Equations (28)–(33) form the generic HMM discretization of (27), each scheme of the family being obtained by making specific choices of the stabilization matrices $\mathbb{B}_{K,i}$ and of the numerical convection method, described by the flux function \mathbf{F}_c .

5.2. Numerical results. It is quite straightforward to adapt the theoretical study made in [11], using the computations from [2], to see that all the schemes obtained by choosing any of the convective methods described above are convergent, under usual assumptions in the HMM setting on the mesh and stabilization matrices. We would like to present here some numerical results obtained by making different choices of \mathbf{F}_c .

The test case we consider is the classical lid-driven cavity with Reynolds number $\text{Re} = 1000$, using two kinds of grids (made of hexahedral cells), Grid 1 and Grid 2, represented in Figure 6. Note that both grids are distorted, albeit in different ways (Grid 1 has many large cells which are distorted but its small cells are quite regular, whereas this is basically the opposite for Grid 2). The solution to the nonlinear HMM schemes (28)–(33) is approximated using a relaxed Newton method, the linear system at each iteration being solved by the BiCGStab algorithm (with ILU preconditioning).

We give in Figures 7 and 8 the streamlines obtained with the HMM method on both grids, using different choices of discretization for the non-linear convective term (SG stands for Scharfetter-Gummel): the centered discretization with cell values (32), the upwind discretization with cell values corresponding to

$$\mathbf{F}_c^{\mathbf{u}_\sigma \cdot \mathbf{n}}(\mathbf{u}, \mathbf{u}_\mathcal{E})_{K,\sigma} = (\mathbf{u}_\sigma \cdot \mathbf{n}_{K,\sigma})^+ \mathbf{u}_K - (\mathbf{u}_\sigma \cdot \mathbf{n}_{K,\sigma})^- \mathbf{u}_L$$

and the Scharfetter-Gummel discretization with cell values given by

$$\mathbf{F}_c^{\mathbf{u}_\sigma \cdot \mathbf{n}}(\mathbf{u}, \mathbf{u}_\mathcal{E})_{K,\sigma} = \frac{1}{d_\sigma} (A(d_\sigma \mathbf{u}_\sigma \cdot \mathbf{n}_{K,\sigma}) \mathbf{u}_K - A(-d_\sigma \mathbf{u}_\sigma \cdot \mathbf{n}_{K,\sigma}) \mathbf{u}_L).$$

The upwind method appears to be a bad choice on both grids: too much numerical diffusion is added to the scheme, and the obtained approximate solution does not clearly exhibit the expected behaviors. The centered choice gives a quite good solution on Grid 1, but seems to strongly suffer from the peculiar distortion of Grid

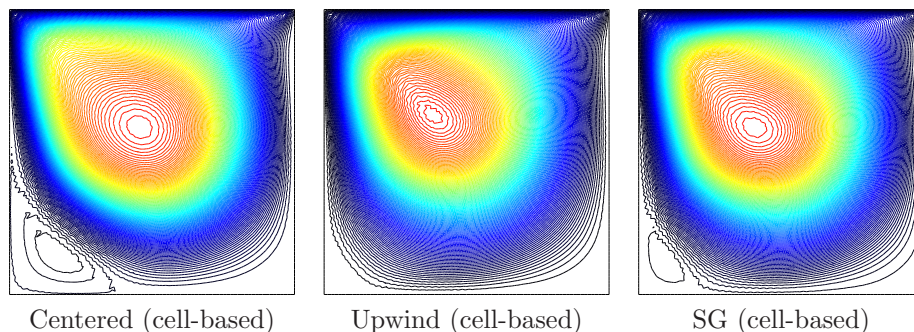


FIGURE 7. Comparison of different choices of discretization of the non-linear convective term in Navier-Stokes equations, for the lid-driven cavity test case on Grid 1.

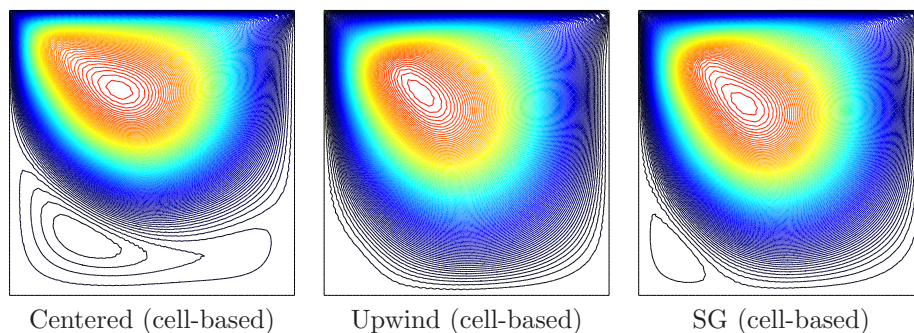


FIGURE 8. Comparison of different choices of discretization of the non-linear convective term in Navier-Stokes equations, for the lid-driven cavity test case on Grid 2.

2 on which the solution it provides can be considered worst (albeit in an opposite way) than the solution given by the upwind method. The solution provided by the Scharfetter-Gummel discretization is not very good, but still better than the one given by the upwind scheme and, above all, seems more “stable” with respect to the distortions of the grids: on the contrary to the centered scheme, the solution of the Scharfetter-Gummel technique on both grids are similar and more or less exhibits some expected behavior of this test-case.

Figure 9 show some approximated solutions obtained using the edge-based variants of the centered and Scharfetter-Gummel discretizations. These results, compared with the previous solutions obtained using the same methods with only the cell unknowns, seem to indicate that the use of the edge-based discretizations for the nonlinear term in Navier-Stokes equations is not as interesting as for (2) in the case of a discontinuous anisotropic tensor (cf Section 4.2.1 and Figure 4).

6. Conclusion. We presented some discretizations of convection-diffusion equations based on the HMM method, a family of schemes for diffusion operators which generalizes the Hybrid Finite Volume, the Mimetic Finite Difference and the Mixed Finite Volume schemes. The HMM method has several possible interpretations, in

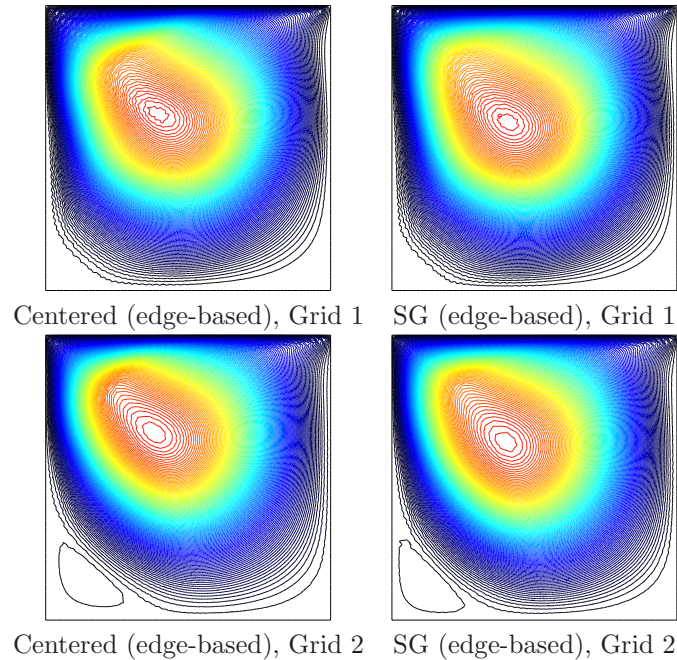


FIGURE 9. Numerical results on the lid-driven cavity test case for the edge-based variants of the discretizations of the non-linear convective term.

particular one from a Finite Volume point of view and one from a Mixed Finite Element point of view, and we used these different presentation of the method to infer several possible discretizations of the convective-diffusive model problem, using well-known techniques from the Finite Volume or Mixed Finite Element literature.

We gave some numerical tests with heterogeneous and anisotropic diffusion tensors, which showed some expected behaviors (order 2 convergence on the unknown for “centered” discretizations of the convective term, order 1 convergence but much better stability in convective regime for “upwind” or stabilized discretizations); we also noticed that the Scharfetter-Gummel method, using the right scaling, appears to be an “optimal” choice in the sense that it automatically adjusts the quantity of numerical diffusion needed to stabilize the method in convective regime, while retaining an order 2 convergence in diffusive regime. Moreover, some numerical tests we provided seem to prove that, in presence of heterogeneity and anisotropy, it is best to use the edge unknown, rather than the cell unknown on the other side of the edge, when computing the numerical convective flux through an edge of a cell.

We wrote the adaptation of the HMM method to the Navier-Stokes equations, which involves a diffusive and a convective term, albeit in a quite different framework than in the case of a simple scalar convection-diffusion equation. We gave some numerical results in the classical lid driven cavity test case, which indicate that, on the contrary to what we noticed for the scalar convection-diffusion equation, the Scharfetter-Gummel method seem to be sometimes less precise than the usual centered discretization for the convected velocity, but also more stable with respect

to the grid distortions. Similarly, the use of the edge unknown in this discretization appears perhaps less useful than in the case of scalar heterogeneous anisotropic convection-diffusion processes.

REFERENCES

- [1] L. Beirão da Veiga and G. Manzini, *A higher-order formulation of the mimetic finite difference method*, SIAM J. Sci. Comput., **31** (2008), 732–760.
- [2] L. Beirão da Veiga, J. Droniou and G. Manzini, *A unified approach to handle convection terms in mixed and hybrid finite volumes and mimetic finite difference methods*, to appear in IMA Journal of Numerical Analysis.
- [3] F. Brezzi, K. Lipnikov and M. Shashkov, *Convergence of the mimetic finite difference method for diffusion problems on polyhedral meshes*, SIAM J. Numer. Anal., **43** (2005), 1872–1896.
- [4] F. Brezzi, K. Lipnikov and V. Simoncini, *A family of mimetic finite difference methods on polygonal and polyhedral meshes*, Math. Models Methods Appl. Sci., **15** (2005), 1533–1551.
- [5] A. Cangiani, G. Manzini and A. Russo, *Convergence analysis of a mimetic finite difference method for general second-order elliptic problems*, SIAM J. Numer. Anal., **47** (2009), 2612–2637.
- [6] C. Chainais-Hillairet and J. Droniou, *Finite volume schemes for non-coercive elliptic problems with Neumann boundary conditions*, IMA Journal of Numerical Analysis, 2009. Doi: 10.1093/imanum/drp009.
- [7] C. Chainais-Hillairet and J. Droniou, *Convergence analysis of a mixed finite volume scheme for an elliptic-parabolic system modeling miscible fluid flows in porous media*, SIAM J. Numer. Anal., **45** (2007), 2228–2258.
- [8] E. Chénier, R. Eymard and R. Herbin, *A collocated finite volume scheme to solve free convection for general non-conforming grids*, J. Comput. Phys., **228** (2009), 2296–2311.
- [9] J. Droniou, R. Eymard, T. Gallouët and R. Herbin, *A unified approach to mimetic finite difference, hybrid finite volume and mixed finite volume methods*, Math. Models Methods Appl. Sci. (M3AS), **20** (2010), 265–295.
- [10] J. Droniou and R. Eymard, *A mixed finite volume scheme for anisotropic diffusion problems on any grid*, Numer. Math., **105** (2006), 35–71.
- [11] J. Droniou and R. Eymard, *Study of the mixed finite volume method for stokes and navier-stokes equations*, Numer. Meth. P. D. E., **25** (2009), 137–171.
- [12] R. Eymard, T. Gallouët and R. Herbin, *Finite volume methods*, In “P. G. Ciarlet and J.-L. Lions, editors, Techniques of Scientific Computing, Part III,” Handbook of Numerical Analysis, VII, pages 713–1020, North-Holland, Amsterdam, 2000.
- [13] R. Eymard, T. Gallouët and R. Herbin, *Discretisation of heterogeneous and anisotropic diffusion problems on general non-conforming meshes, sushi: A scheme using stabilisation and hybrid interfaces*, to appear in IMAJNA, see also <http://hal.archives-ouvertes.fr/docs/00/21/18/28/PDF/suchi.pdf>, 2008.
- [14] R. Ewing, T. Russel and M. Wheeler, *Simulation of miscible displacement using mixed methods and a modified method of characteristics*, in Proceedings of the 7th SPE Symposium on Reservoir Simulation, Dallas, TX, Paper SPE 12241, Society of Petroleum Engineers, 1983, 71–81.
- [15] D. T. F. Russell, *Finite elements with characteristics for two-component incompressible miscible displacement*, in Proceedings of the 6th SPE Symposium on Reservoir Simulation, New Orleans, Paper SPE 10500, Society of Petroleum Engineers, 1982, 123–135.
- [16] L. Scharfetter and H. K. Gummel, *Large signal analysis of a silicon Read diode*, IEEE Trans. on Elec. Dev., **16** (1969), 64–77.
- [17] H. Wang, D. Liang, R. E. Ewing, S. L. Lyons and G. Qin, *An approximation to miscible fluid flows in porous media with point sources and sinks by an Eulerian-Lagrangian localized adjoint method and mixed finite element methods*, SIAM J. Sci. Comput., **22** (2000), 561–581.

Received January 2010; revised April 2010.

E-mail address: droniou@math.univ-montp2.fr